Comparative Molecular Dynamics Study of Lipid Membranes Containing Cholesterol and Ergosterol

Jacek Czub and Maciej Baginski
Department of Pharmaceutical Technology and Biochemistry, Faculty of Chemistry, Gdansk University of Technology, Gdansk, Poland

ABSTRACT Sterol molecules are essential for maintaining the proper structure and function of eukaryotic cell membranes. The influence of cholesterol (the principal sterol of higher animals) on the lipid bilayer properties was extensively studied by both experimental and simulation methods. In contrast, the effect of ergosterol (the principal fungal sterol) on the membrane structure and dynamics is much less recognized. This work presents the results of comparative molecular dynamics simulation of the hydrated dimyristoylphosphatidylcholine bilayer containing ~25 mol % of cholesterol or ergosterol. A detailed analysis of the molecular properties (e.g., bilayer thickness, lipid order, diffusion, intermolecular interactions, etc.) of both sterol-induced liquid-ordered membrane phases is presented. Presence of sterols in the membrane significantly changes its property, especially fluidity and molecular packing. Moreover, in accordance with the experiments, our calculations show that, compared to cholesterol, ergosterol has higher ordering effect on the phospholipid acyl chains. This different influence on the properties of the lipid bilayer stems from differences in conformational freedom of sterol side chains. Additionally, obtained models of lipid membranes containing human and fungal sterols, constituting the result of our work, can be also utilized in other chemotherapeutic studies on interaction of selected ligands (e.g., antifungal compounds) with membranes.

INTRODUCTION

Cholesterol (Chol), an important molecule that occurs in significant concentrations (30–50 mol %) in the majority of animal cell membranes, is known to play a fundamental role in maintaining their proper structure and function (1,2). It is well established that the biological importance of this sterol arises particularly from its ability to modulate the physicochemical properties of lipid bilayer. A large amount of experimental and theoretical work showed that Chol, for instance, broadens and eventually abolishes the main phase transition of phospholipid bilayers, increases the membrane mechanical strength, and decreases the permeability of the bilayer to small molecules (for review, see (3,4)). At the molecular level, Chol is known to effectively order the hydrocarbon chains of adjacent lipid molecules, but at the same time, it preserves the relatively high degree of their lateral mobility (5,6). Apparently, as a consequence of thereof, lipid membranes containing Chol may simultaneously satisfy radically different biological requirements such as constituting a mechanically strong and nonpermeable cell-protecting barrier, while also providing a fluid environment for embedded proteins. Recently, much attention has been paid to the involvement of Chol in formation of the so-called liquid-ordered (*lo*) phase in mixed bilayers. The *lo* domains that are enriched in Chol and saturated long-chained lipids were shown to be characterized by a high conformational order and, interestingly, by essentially higher lateral mobility compared to a gel phase (7). It is postulated that the natural *lo* microdomains (so-called rafts), which, apart from Chol, also contain sphingolipids, saturated glycerophospholipids, and certain proteins, may participate in many cellular processes including signal transduction, protein sorting and trafficking, immune response, bacterial invasion, viral entry, and budding (8–11).

Similarly to Chol in higher animal membranes, ergosterol (Erg) is a principal sterol in fungi, certain protozoans, and insects such as *Drosophila* (12,13). As opposed to many studies concerning Chol-containing membranes, the effect of Erg on structure and dynamics of lipid bilayers has not been investigated so extensively. However, several reports demonstrate that the ability of Erg molecules to order saturated lipid chains is substantially higher in comparison with Chol (14–16). Recently, it was also shown that Erg, similarly to Chol, can promote the separation of liquid-crystalline DPPC bilayer into coexisting *lo* and liquid-disordered (*ld*) phases (17). Moreover, applying detergent insolubility methods, it was found out that lipid rafts containing Erg, specific fungal sphingolipids, and glycophosphatidylinositol-anchored proteins, are likely to exist in plasma membranes of *Saccharomyces cerevisiae* and *Drosophila* (18,19).

Despite many previous efforts, the relationship between a chemical structure of different sterols and their influence on the lipid bilayer properties has not been yet precisely determined (20,21). Unraveling such a relation would be very important for understanding the reason of an unusual complexity of the sterol biosynthesis pathways, which have been furthermore hypothesized to recapitulate the sterol structure evolution (22,23). Explaining this dependence would also be of primary importance for designing new

Submitted August 18, 2005, and accepted for publication November 16, 2005.

Address reprint requests to Maciej Baginski, Dept. of Pharmaceutical Technology and Biochemistry, Faculty of Chemistry, Gdansk University of Technology, 11/12 Narutowicza St, 80-952 Gdansk, Poland. Tel.: 48-58-347-1596; Fax: 48-58-347-1144; E-mail: maciekb@hypnos.chem.pg.gda.pl.

0006-3495/06/04/2368/15 $2.00

doi: 10.1529/biophysj.105.072801

drugs targeting pathogens containing sterols other than Chol (especially Erg) in their cell membrane.

Molecular dynamics (MD) simulations of lipid membranes have been carried out for over a decade and have become a well-established approach, often providing their molecular interpretation, which proved to be a valuable supplement of the experimental methods (24–26). Due to a high resolution, the MD technique, contrary to the experimental methods, offers a detailed insight into processes and interactions occurring at the atomic level, which underlie the properties observed in a larger scale. Until the present day, many valuable MD simulations of one-component as well as mixed lipid bilayers have been performed. Specifically, the effect of Chol on the phospholipid membrane properties visible on MD-accessible time- and length-scale has been extensively studied (27–31). These works resulted in successful reproducing of numerous measurable properties of Chol-containing membranes, including the order parameter, the area per lipid molecule, the lateral diffusion constant, and the electron density profile across bilayer. Furthermore, the unique possibilities of the MD method facilitated a better interpretation of the different Chol-induced effects as well as provided additional precise data on, e.g., intermolecular interactions (charge pairs, hydrogen-bonding patterns, etc.) in simulated systems. The only MD study on the Erg-doped membrane was performed by Smondyrev and Berkowitz (32). The authors simulated mixed bilayers composed of 2,3-dimiristoyl-D-glycero-1-phosphorylcholine (DMPC) and three different sterols: Chol, its biosynthetic precursor, lanosterol, and Erg. This study, however, did not show any substantial differences between properties of the Chol- and Erg-containing systems, probably because the sterol concentration (11.1 mol %) was too low (below typical physiological level).

In this work, we utilize the MD technique to elucidate how the small structural differences between Chol and Erg molecules (Fig. 1) result in varied modulation of the lipid membrane properties. To the best of our knowledge, the present simulation of DMPC bilayers containing ~25 mol % of both sterols is the first one to reproduce the experimental difference in the molecular order of the Chol- and Erg-induced *lo* phases. This agreement enables us to discuss and point out the most probable reasons for the observed differences.

It is also worth mentioning that a different modulating influence of Chol and Erg on the lipid bilayer physicochemical properties is often regarded as a base of a selective toxic effect of polyene macrolide antibiotics (e.g., amphotericin B or nystatin) (33,34). These channel-forming compounds are more effective in membranes with Erg (fungi) than in those with Chol (mammals), and therefore can be used as antifungal drugs. Recent reports indicate that ordered lipid domains enriched with sterols can be the actual target of amphotericin B and other polyenes (35). Thus, our comparison of model *lo* lipid phases containing Chol and Erg may help us to further understand the molecular mechanism of action of these important antifungal drugs. Moreover, the prepared hydrated sterol systems can be used in future studies on interaction of polyenes and some other membrane-active agents (e.g., antimicrobial peptides) with lipid bilayers.

METHODS

Molecular models

The systems simulated herein were constructed from the liquid-crystalline DMPC bilayer model made available by P. Tieleman from the University of Calgary (Canada) on his web page (*http://moose.bio.ucalgary.ca*). This type of phospholipid molecule was selected to facilitate a comparison of our results with the previous experimental and computational studies on the phosphatidylcholine/Chol (Erg) systems (5,14,32,36,37). Additionally, because the systems obtained in the reported study are planned to be utilized in the future for the calculations involving drug-lipid bilayer interactions, we intended to maintain consistency in a series of our earlier and present works by choosing DMPC (38–40).

The original DMPC membrane patch was built of 64 lipid molecules in each leaflet. For the purposes of the current simulation, the model was

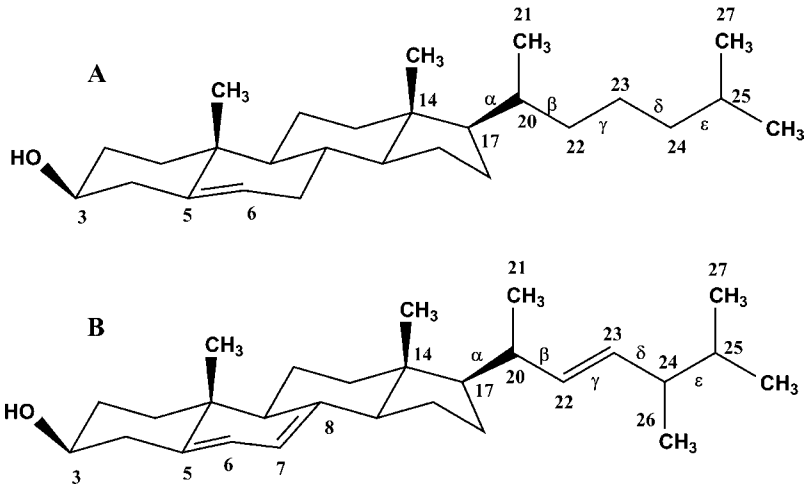

FIGURE 1 Structure of cholesterol (*A*) and ergosterol (*B*) molecules. Definitions of distinguished dihedral angles are the following: $\alpha \equiv$ (C14–C17–C20–C22), $\beta \equiv$ (C17–C20–C22–C23), $\gamma \equiv$ (C20–C22–C23–C24), $\delta \equiv$ (C22–C23–C24–C25), and $\varepsilon \equiv$ (C23–C24–C25–C27).

extended by introducing into the membrane 42 sterol molecules. As a result, two mixed bilayers, each containing 24.7 mol % of Chol or Erg, respectively, was obtained. The molar fraction of sterols used here is similar to the one applied in the related experimental studies (14,16). Additionally, the phosphatidylcholine/Chol (Erg) phase diagrams (7,17) indicate that the used molar fraction and applied simulation conditions should maintain the membranes in the liquid-ordered state.

The initial geometries for Chol and Erg were taken from crystal structures (41,42). Only Chol and Erg molecules with extended side chains were used for the model's elaboration, according to the previous conformational analysis (43). The insertion of sterols into the bilayer was performed in six subsequent stages. At each step, seven randomly selected DMPC molecules were translated in the *x*,*y* plane (parallel to the bilayer surface) to the close proximity of the nearest bilayer edge and fitted (to avoid overlapping) to the geometry of boundary molecules by applying proper rigid-body rotations. The same number of the sterol molecules were placed in the formed free spaces in such a way that their longest principal axes were roughly parallel to the membrane normal (the *z* axis). The length of the two sterols in their extended conformations is very similar; therefore, we positioned both types of inserted sterol molecules at the same membrane level, with their hydroxyl groups placed approximately between the average positions of the carbonyl and phosphate groups of DMPC. At each stage, the modified structure was energy-minimized to remove bad van der Waals contacts and shortly (0.5–1.0 ns) equilibrated in NPT ensemble after extending slightly the *x* and *y* dimensions of the simulation cell. The whole procedure resulted in obtaining two membrane systems with sterol molecules distributed homogeneously in the DMPC matrix. The same number of sterols in both bilayer leaflets was preserved.

During the system preparation 1623 water molecules were added to the already existing ones, so the total number of waters in both simulations was equal to 5278. This was done to better separate the bilayer surfaces in periodic boundary conditions and, therefore, more adequately describe the unilamellar membrane. Such a bilayer type is more physiologically relevant, and usually used in the experimental studies of drug-membrane interaction. As mentioned above, we are planning to carry out a series of comparative MD simulations employing the same lipid bilayer core and different ligands, and thus the other reason for increasing volume of aqueous phase was to create space for future model rebuilding (e.g., placing ions or drug molecules in water lamella, etc.).

For comparison purposes, we also performed a simulation of original pure DMPC bilayer with a proper number of water molecules added.

Simulation details

All the energy minimizations and MD simulations were carried out using GROMACS package (44). The topology and force-field parameters for DMPC molecules were based on the commonly used united-atom parameter set for DPPC (45). This force field is a consistent combination of different parameterizations, designed especially for reproducing the measurable membrane properties. The 6–12 potential parameters and bonded parameters for Chol and Erg were taken from standard GROMACS *ffgmx* force. Similarly to DMPC molecules, the united-atom approach was applied for all nonpolar CH_n groups in both sterols. As a result, only polar hydrogen atoms of 3β-hydroxyl groups were kept explicitly. Because the semiempirical (46) and ab initio (unpublished results) quantum mechanical calculations carried out by us showed that the distribution of electrostatic potential around the polar head of Chol and Erg molecules is very similar, we used the same partial charges for both molecules. For the purpose of compliance with the previous simulations of phosphatidylcholine/Chol systems (30,31), we applied nonzero charges only to the three headgroup atoms of the sterol molecules (values were the same as in the cited works: $+0.40e$ on hydrogen, $-0.54e$ on oxygen, and $+0.14e$ on C3 carbon atoms). It is worth mentioning that the same parameter set for Chol was used in previous simulations of phosphatidylcholine/Chol systems and was successful in reproducing macroscopic properties of studied membranes (30,31). Moreover, as a consequence of similar chemical structure of Chol and Erg, the differences between parameter sets applied for sterol molecules were only slight. Therefore, we can also expect that Erg parameterization was consistent with the force field employed for DMPC molecules. The single-point-charge model (47) was chosen to describe water molecules.

The potential energy function used in our calculations includes all typical intra- and intermolecular components. In accordance with the force field chosen for DMPC molecules, bond rotations in their acyl chains were described by the Ryckaert-Bellemans potential (the corresponding 1–4 neighbors were excluded from nonbonded interactions). The 1–4 electrostatic interactions and the 1–4 Lennard-Jones interactions within the headgroup of DMPC molecules were scaled by the factor of 0.5 and 0.125, respectively. Three-dimensional periodic boundary conditions were applied to eliminate edge effects. Electrostatic interactions were estimated by means of the smooth particle-mesh Ewald summation method (48), with direct space cutoff of 0.9 nm, and fast Fourier-transform grid spacing of ~0.1 nm in all three dimensions. The Lennard-Jones interactions within 0.9 nm distance were evaluated every MD step and interactions between 0.9 and 1.2 nm were evaluated every 10 steps. To make it possible to use a longer time step, all covalent bonds in the system were constrained to their reference values with the LINCS algorithm for phospholipid and sterol molecules and with the SETTLE scheme for water molecules (49,50).

All MD simulations were performed by using the leap-frog Verlet algorithm with an integration step of 2 fs at constant pressure and temperature (NPT ensemble). The temperature and pressure were maintained stable at ~300 K and 1 bar by means of the Berendsen weak coupling method (51), with time constants of 0.1 and 1.0 ps, respectively. To counteract a possible formation of temperature gradients, temperature coupling was applied separately to the solvent and lipid molecules. Pressure was scaled independently in all three space directions. The pair-list for short-range nonbonded interactions was updated every 10 MD steps. All three systems (pure DMPC and both DMPC/sterol systems) were simulated for 35 ns. The last 25 ns of each run were then taken for calculating averages. The total energy, its components, and dimensions of the simulation cell were monitored, and the equilibration time employed seemed to be sufficient to obtain reasonable convergence of most properties of our interest (data not shown).

RESULTS AND DISCUSSION

Molecular dynamics study and analysis of 25-ns simulation trajectories of DMPC lipid membranes containing ~25 mol % cholesterol or ergosterol were performed. We focused our analysis not only on gaining a deeper insight into the molecular properties of phospholipid membranes containing sterols, but also on comparison of both types of membranes. Chol and Erg are the most important sterols present in mammalian and fungal cell membranes, respectively. Therefore, our results and the obtained membrane models can also be used for studies of interactions between different ligands (including potential drugs) and cell membranes.

For clarity, Results and Discussion was divided into the subsections presented below.

Condensing effect

To illustrate a commonly known condensing effect exerted on lipid bilayers by sterols, we calculated the average areas per lipid molecule in all three simulated systems. The interfacial area per molecule can be readily obtained in single-component systems, where it is usually calculated by

dividing the total area by the number of molecules forming the surface. The mean area per DMPC molecule determined in that way from the simulation of pure system was 0.618 ± 0.0083 nm^2. This value generally reflects the experimental data for liquid-crystalline DMPC bilayer ranging from 0.597 to 0.617 nm^2, dependent upon the method used (52,53). It also indicates that a simple shortening of hydrocarbon tails in the Berger's DPPC parameterization may be sufficient to obtain a reasonable model of DMPC bilayer.

Contrary to homogenic systems, dividing the surface membrane area among components in mixed systems (e.g., phospholipid/sterol bilayer) is quite ambiguous (30,54). Due to the fact that our main intention was to compare the influence of both sterols on membrane properties, the choice of the method to distribute the area between DMPC and sterols was of rather secondary importance. All of the methods should allow for at least qualitative comparison of sterol's condensing action on the phospholipid environment. It has been recently shown (30) that reasonable values of the mean area per phospholipid in sterol-containing membranes can be achieved by applying the formula

$$A_{PC} = \frac{2A}{N_{PC}}\left(1 - \frac{N_{st}V_{st}}{V - N_wV_w}\right), \quad (1)$$

where A and V are the x,y area and the total volume of the simulation cell, respectively; N_{PC}, N_{st}, and N_w are the total numbers of particular molecules in the system (phospholipid, sterol, and water, respectively); V_w constitutes the volume of water molecule; and V_{st} is the volume occupied by the sterol molecule. The above equation was derived on the assumption that there are no free volumes (holes) in the system, so the whole space is divided among individual molecules. To effectively apply the above formula, it was also necessary to assume that the volume of a relatively rigid sterol molecule inside the bilayer is independent of the system composition and is equal, for example, to the experimental value found for sterol in the crystal structure. As it was done before (32), for the purposes of our analysis, we initially assumed that the molecular volume of both sterols is the same and is equal to a value of 0.593 nm^3 estimated for Chol from the crystal data (30). The volume occupied per one SPC water molecule at 300 K (V_w = 0.0312 nm^3) was calculated via a separate simulation of pure water with all conditions the same as in the membrane simulations. The average value of the x,y area and the total volume in the DMPC/Chol system were calculated to be 38.321 ± 0.322 nm^2 and 320.781 ± 0.509 nm^3, respectively (analogical values for the DMPC/Erg systems were equal to 36.336 ± 0.232 nm^2 and 320.599 ± 0.501 nm^3). Finally, the obtained average areas per DMPC were 0.503 ± 0.0067 and 0.476 ± 0.0057 nm^2 for the systems containing ~25 mol % of Chol and Erg, respectively. Therefore, comparing the values for mixed (DMPC/sterol) and pure (DMPC) systems, it is evident that both sterols have strong condensing ability. However, the effect induced by Erg is significantly stronger compared to that produced by Chol. On the other hand, the estimated molecular area of DMPC in the DMPC/Erg system is only slightly higher than the experimentally determined area of pure DMPC in the gel phase (0.472 ± 0.05 nm^2) (55). One might expect that our value should be higher due to observed significant lateral diffusion and disorder of the DMPC molecules in the studied system. The underestimation of molecular area of DMPC in the DMPC/Erg system may stem from our initial assumption that the molecular volume of Erg is equal to the volume of Chol. In fact, the presence of a double bond in the Erg side chain should restrict the extent of conformational changes within this region and, consequently, should result in decreasing of the effective volume of the molecule with respect to Chol (see also Sterol Structure and Orientation).

To estimate relative difference of sterol molecular volumes arising from diverse dynamic behavior of the side chains, a procedure was applied in which the MD structures of individual sterol molecules were overlapped using C3, C5, C8, and C17 carbon atoms of the ring systems as the fitted atoms. Because the phospholipid wobbling motion take place on a nanosecond timescale (56), the sterol geometries were sampled every 100 ps through the period of 5 ns. The volumes of the obtained atom sets were then calculated analytically using standard values of van der Waals radii and averaged over all molecules of given sterol type. Finally, the Erg/Chol volume ratio was calculated to be 0.87, which confirms the presumed difference in the effective volume of both studied sterols. Taking the crystallographic volume of Chol as the reference value, we estimated the relative volume of the Erg molecule (0.516 nm^3) and used it in Eq. 1 to obtain the corrected area per DMPC in the DMPC/Erg system (0.489 ± 0.0057 nm^2). As it was expected, new calculated value is greater then previously estimated one; however, the general conclusion that Erg causes stronger condensation of phospholipids, still seems to be justified. Thus, we may furthermore expect that Erg molecules are able to increase the order in phospholipid bilayer to a higher degree compared to Chol (see also Ordering of Acyl Chains). This observation is consistent with a number of experimental results, indicating that Erg-containing membranes are more rigid and tightly packed/ordered than their Chol equivalents (15,20).

We also estimated the average area occupied by sterol molecules in both simulated systems. To this end, the formula was used (30),

$$A_{st} = \frac{2A - N_{PC}A_{PC}}{N_{st}}, \quad (2)$$

where the meaning of symbols is the same as in Eq. 1. The obtained values are 0.292 ± 0.035 nm^2 and 0.240 ± 0.028 nm^2 for Chol and Erg, respectively (the corrected value of A_{PC} equal to 0.489 ± 0.0057 nm^2 was used in the DMPC/Erg system). Since the steroid nuclei of both sterols have very similar cross-sections in the x,y plane, one may presume

that the difference observed in the average molecular area arises from dynamical properties, i.e., different off-axial mobility of sterol core and hydrocarbon side chain, higher in the case of Chol. The value of the area per Chol is enclosed in the range previously determined in the same way for Chol in DPPC and DLPC bilayers (0.26 and 0.31 nm^2, respectively) (31). This confirms an effect of the monotonic increase of the area occupied by sterol molecule with decreasing phospholipid chain length. This trend seems to result from shortening of the phospholipid acyl chains with respect to the Chol hydrophobic length. It should also be noted that the employed estimation procedure appears to be better suited for bilayers made of shorter phospholipids, where the assumption that there is no free volume could, to a lesser extent, overestimate the volume and the area per phospholipid. Hence, values of the area per Chol obtained in DMPC and DLPC systems are closer to the previous experimental and computational data (32,41).

The overall DMPC bilayer condensation induced by introduction of 24.7 mol % of Chol and Erg, calculated by subtracting the whole area in sterol-containing systems from the area of pure DMPC membrane, equaled to ~0.02 and ~0.04 nm^2/(1 DMPC molecule), respectively. As it was shown above, the observed difference can be considered as arising from two effects: 1), stronger Erg ability to pack phospholipid molecules; and 2), a smaller average surface area occupied by this kind of sterol.

Transverse structure

To provide insights into the transverse structure of the examined systems, the average electron density profiles across the bilayer were calculated and are plotted in Fig. 2. The plots have all the typical features observed in diffraction experiments, including two pronounced peaks corresponding approximately to the position of the electron dense phosphate groups and a minimum in the middle of the bilayer (53,57). Furthermore, the calculated EDP of pure DMPC bilayer seems to be in fairly good quantitative agreement with the x-ray diffraction data also presented in Fig. 2 (57). There are, however, some discrepancies, especially concerning the position and width of the lipid headgroup peaks, which in the computed profile are shifted a little toward the bilayer center and are also significantly broader. Nevertheless, it seems that the quality of EDP reproduction obtained in the case of pure DMPC makes the comparison of the sterol-containing systems more reasonable. The distance between the maxima (head-to-head spacing, D_{HH}) is often used as a quantitative measure of the membrane thickness (53). It can be seen that calculated thickness of pure DMPC membrane (~3,31 nm) is rather close to experimental value of ~3.50 nm (57). Fig. 2 shows that the presence of ~25 mol % of both studied sterols in the membrane substantially increases its thickness. One can also see that the alteration in bilayer thickness induced by Erg (an increase from 3.31 to 4.15 nm) is distinctly higher compared to the one induced by Chol (an increase to 3.93 nm). Structural changes in the membrane hydrocarbon region caused by sterol addition are also more distinct in the case of Erg. These changes, manifested especially by the appearance of the flat regions between the peaks and the minimum of the density plots together with the density reducing in the middle of the bilayer, are characteristic of the membranes in the liquid-ordered (*lo*) bilayer phase. In Fig. 3 we separated the total electron density profiles of the sterol systems into contributions due to the different types of molecules, i.e., water, DMPC, and sterols. In addition, the sterol profiles were divided into its components from the fused ring system and from the hydrocarbon side chain. These plots clearly confirm

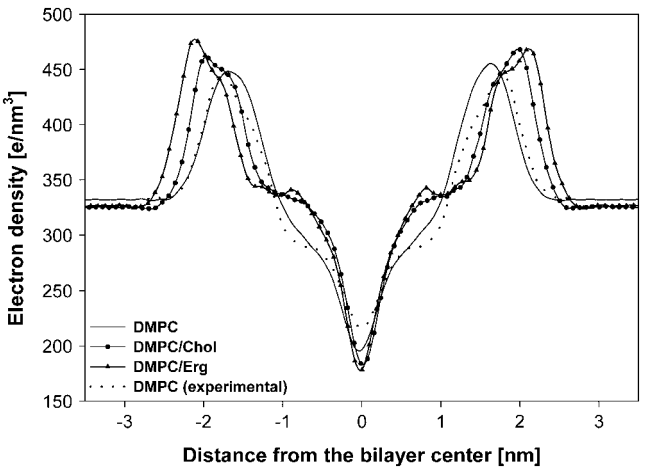

FIGURE 2 The electron density profiles of the simulated systems along the bilayer normal. Experimental profile for pure DMPC bilayer is taken from Kucerka et al. (57).

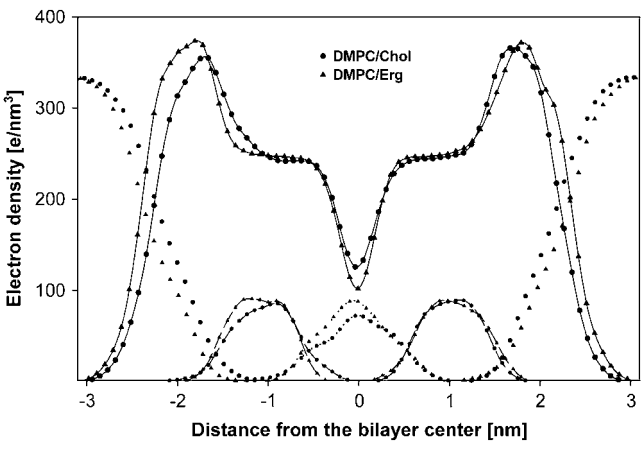

FIGURE 3 Individual components of the electron density profiles along the bilayer normal in the simulated systems: DMPC molecules (*solid line*), sterol ring system (*dashed line*), sterol side chain (*dotted line*), and water molecules (*symbols only*; *no line*).

the observation that, in comparison with Chol, Erg has a greater ability to increase the thickness of the DMPC bilayer. All visible differences in the electron density distribution for both sterol-containing systems are more distinct in the hydrophobic core of the membranes. The penetration of water into the bilayer as well as the width of the membrane/water interface region seems to be very similar in both systems. On the contrary, the density increase in the phospholipid chain region and the extent of leaflet separation do depend on the molecular structure of the sterol present. It is worth noticing that these effects, more evident in the DMPC/Erg system, were previously found to correlate with increasing Chol concentration in the phospholipid bilayer (30,54). This observation indicates again that Erg has stronger ability to stiffen bilayers composed of at least saturated phospholipids, such as DMPC. The density plots for Chol and Erg differ mainly in their side-chain parts, with the distribution corresponding to the side chain of Chol significantly more dispersed, suggesting higher off-axial mobility of the Chol side chain. Since the distributions of the ring systems of both sterols are similar, one can propose that the difference in side-chain conformational freedom may be crucial for different lipid-ordering effect of the studied molecules.

To characterize the structure of examined systems in more detail, we also calculated transverse electron density distributions of the selected functional groups from DMPC and sterols. The resulting plots, which present values averaged over the two membrane leaflets, are presented in Fig. 4. It can be seen that, in both systems, the hydroxyl groups of sterols are solvated to a similar extent and are located at approximately the same distance from the bilayer center as the carbonyl groups of DMPC, suggesting relatively strong and preferential interaction between these groups. The distributions of the particular groups of atoms in the DMPC/Chol system are noticeably broader than the corresponding peaks in the DMPC/Erg bilayer. The detected difference, which concerns the groups both from DMPC (e.g., phosphate group) and from sterols (e.g., hydroxyl group), seems to indicate that in the Erg-containing membrane the transverse mobility of components and thickness fluctuations are considerably smaller compared to the second analyzed system. Regardless of the sterol present, water molecules penetrate into the bilayer up to the carbonyl groups and the relative location of the peaks associated with the trimethylammonium, $N(CH_3)_3^+$, and phosphate groups, PO_4^-, is also very similar. Thus, Fig. 4 supports prior observations that the different molecular structure of both sterols has a minor effect on the organization of the water/bilayer interface. Considering the bilayer thickness, we can see that the observed difference between both membranes is entirely independent of the different width of the hydrophobic region, because the relative position of the carbonyl group and both charged groups in the two simulated systems is almost the same. In the case of the Erg-containing membrane, separation of both leaflets is more distinct (see the density of the terminal methyl group of DMPC in Fig. 4). In comparison with Chol, Erg molecules are more strongly extended along the bilayer normal (see the density of the terminal isopropyl group of both sterols).

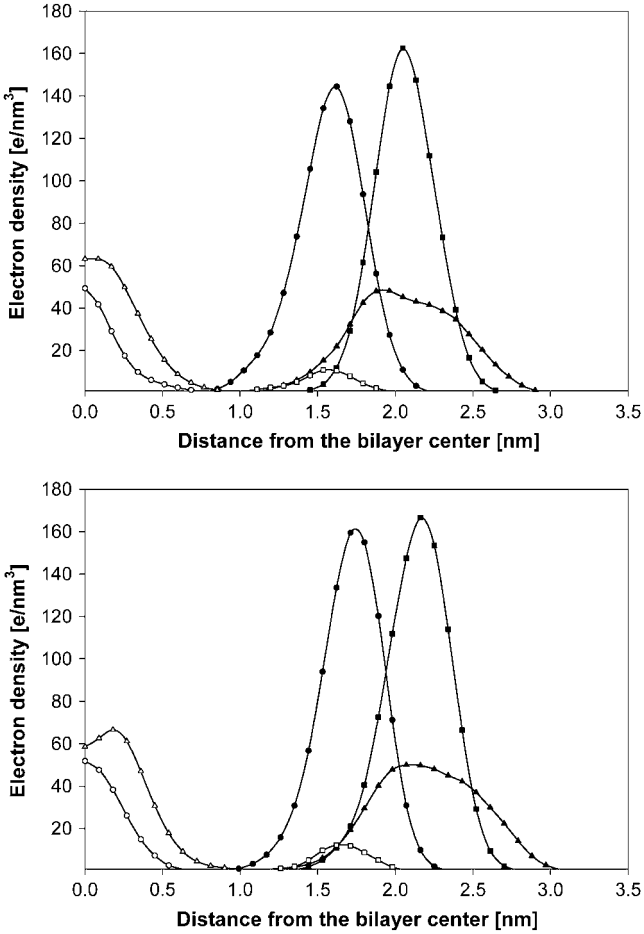

FIGURE 4 Electron densities of various groups across the DMPC/Chol (*a*) and DMPC/Erg (*b*) bilayer: DMPC trimethylammonium groups (▲), DMPC phosphate groups (■), DMPC carbonyl groups (●), DMPC terminal methyl groups (Δ), sterol hydroxyl groups (□), and sterol terminal isopropyl group (○).

Ordering of acyl chains

The observations presented above, especially the discovered differences in the bilayer thickness and in the average area per DMPC, indicate that Erg has a higher ability to order the phospholipid acyl chains. To verify this result directly, we calculated the order parameter profiles of the DMPC acyl chains. The deuterium order parameter, S_{CD}, is a common measure of the lipid bilayer order obtainable from NMR experiments on a deuterated sample or from MD simulations. For a given lipid methylene group, it may be defined as

$$S_{CD} = \frac{3}{2}\langle \cos\beta \rangle - \frac{1}{2}, \quad (3)$$

where β is the angle between the C–D (or C–H) bond vector and the bilayer normal. Since we employed the united-atom model, to calculate the order parameter in a direct way we had to assume the tetrahedral geometry of all methylene groups. For every methylene group the averaging was done over both C–H bonds, all the lipid molecules, and the simulation time.

The values of S_{CD} obtained separately for the DMPC *sn*-1 and *sn*-2 chains are shown in Fig. 5 as a function of the carbon atom number. The profiles calculated for the pure DMPC bilayer exhibit all typical features of such plots and are in compliant with the experimental data (5,14,58). As it is shown in Fig. 5, the S_{CD} values computed for pure DMPC are fairly close to the measured ones obtained in the temperature of 303 K in the NMR experiments using deuterated lipid samples (58). Particularly, the differences between the calculated and experimental plots are smaller than differences between both profiles obtained for two sterol-containing membranes. All the experimental values are, however, a bit larger (more negative) then corresponding ones from the simulation, suggesting that the force-field parameter set used for the lipid molecules has a tendency to produce a slightly too high conformational disorder in the membrane hydrocarbon interior. This effect is also consistent with the discrepancies noticed before for the electron density profile and the membrane thickness. The difference observed in ordering of the *sn*-1 and *sn*-2 chains was also previously detected in experiment and simulations (5,30) and is attributed to a relative shift of both chains along the *z* axis; methylene groups of the *sn*-2 chain are, on average, located closer to the bilayer surface than the corresponding ones in the *sn*-1 chain. As can be seen, an addition of ~25 mol % of each sterol to the pure DMPC bilayer leads to the increase of the molecular order within the hydrocarbon interior of the membrane (raising of $|S_{CD}|$ values). The values of the order parameter obtained for both sterol-containing membranes indicate that the systems are in the *lo* phase. In a relatively flat region of the profiles (C3–C9) the order parameter of the acyl chains in the Chol-containing membrane is ~1.5 times higher compared to the pure DMPC bilayer, which is in agreement with the values observed in other studies (5,14). Corresponding value for Erg-containing system is equal to ~2.0, denoting that, compared to Chol, the fungal sterol has significantly greater ordering effect on the acyl chains of saturated phospholipid molecules. This conclusion is consistent with the results of several experimental approaches, including direct measurements of S_{CD} in ^{2}H-NMR spectroscopy (14) and estimations made by measuring of steady-state fluorescence anisotropy of a probe molecule (16). The ordering influence of both sterols is especially visible in the middle region of the DMPC acyl chains (C3–C9), where the rigid sterol ring systems reside. It is also worth noticing that the conformational order of the upper and lower parts of the acyl chains in the sterol-containing bilayers is more symmetric compared to the pure DMPC. This symmetrization, observed also in the experiment (14), stems from the similar length of sterol molecules and the acyl chains of DMPC, and does not occur in the case of membranes made of longer lipid molecules, such as DPPC (30). Fig. 5 also shows that incorporation of sterols into the DMPC bilayer additionally widens the difference between the molecular order of both acyl chains.

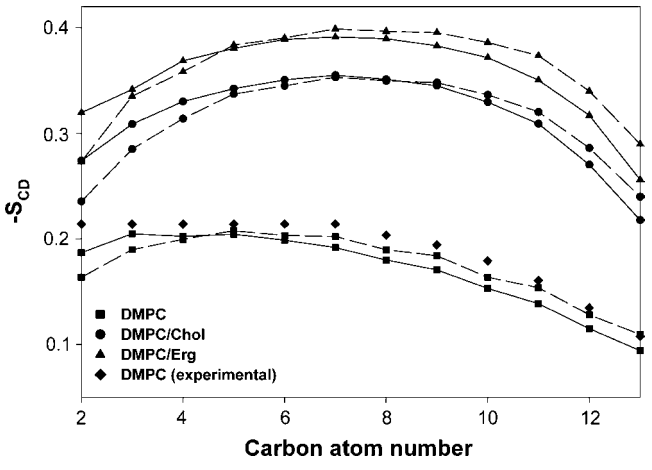

FIGURE 5 Profiles of the deuterium order parameter calculated for the DMPC *sn*-1 (*solid line*) and *sn*-2 (*dashed line*) in the simulated systems. Experimental values averaged over both DMPC acyl chains are taken from Petrache et al. (58).

Sterol structure and orientation

Despite many previous efforts, the relationship between the chemical structure of biologically relevant sterols and their influence on the cell membrane properties still has not been definitely determined (20,22). In an attempt to establish the origin of differences in the effect of Erg and Chol on the micromechanic behavior of the lipid bilayer (especially on its conformational order), we performed a comparison of orientation and structural properties of both sterol molecules in the membrane environment. First, we calculated the average tilt of the sterol molecules with respect to the bilayer normal. Since our earlier analysis suggested that the main reason of the different packing properties of both sterols may arise from the diverse chemical constitution of their side chains, we separately considered the tilt of the plane ring system and the tilt of the short hydrocarbon chain. The tilts were defined as the angles between the membrane normal and the vectors connecting atoms: C17 → C3 and C25 → C17 (see Fig. 1), respectively. The calculated distributions of the tilt angles are presented in Fig. 6. As can be seen, in the case of Chol the average values of both defined angles (19.4° and 28.6°) are significantly higher than for Erg (13.2° and 16.8°). Due to the fact that in the both simulated systems the sterol hydroxyl groups are strongly anchored at the level of the DMPC carbonyl groups (see also Fig. 2 and Table 2), one

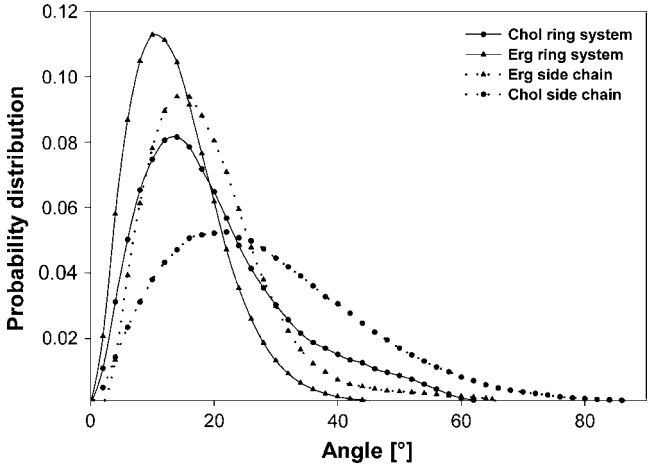

FIGURE 6 Distributions of the sterol tilt angles calculated separately for the sterol ring system and sterol side chains in the simulated systems. Tilts are defined as angles formed between the C17→C3 (*ring system tilt*) or C25→C17 (*side-chain tilt*) vectors and the bilayer normal.

possible reason for the above-mentioned effect consists in the different hydrophobic thickness of the two membranes. The length of both sterol molecules in their extended forms is ~1.6 nm, so that Chol needs to be more tilted to match the hydrophobic thickness of ~1.4 nm corresponding to one membrane leaflet. Erg, in general, does not have to adjust the *z* component of its length to the hydrocarbon phase span, because the hydrophobic thickness of the Erg-containing membrane is greater. On the other hand, the widths of the obtained distributions (Fig. 6) seem to be interconnected with the different conformational order of the two bilayers, being substantially larger for the more disordered Chol-containing membrane. The difference is especially evident for the side-chain region, where, possibly due to the different chemical structure, the probability of a deviation from the membrane normal direction is, in the case of Erg, highly reduced. Taking this fact into consideration, one could propose that the restriction of the rotational freedom of the hydrocarbon chain is the main cause of the Erg's stronger ability to increase the molecular order of the lipid bilayer. The higher global order of the Erg-containing membrane, in turn, additionally limits the overall off-axial mobility of sterol molecules embedded in the *lo* phase.

To further investigate this hypothesis, we computed the distributions of the dihedral angles of the sterol side chains. These values were averaged over all the molecules and the simulation time (Fig. 7). It is evident that the presence of the double bond and the additional methyl group in the Erg side chain (see Fig. 1) strongly influence the geometry of that part of the molecule. The double bond not only completely restricts the rotation of the γ-angle (C20–C22–C23–C24), which in the Chol molecule behaves as in a flexible hydrocarbon chain (higher maximum at 180° and far more lower at 60° and 300°), but also has an effect on the overall structure of the sterol side chain. The two methyl groups (C21 and C26) symmetrically flanking a planar structure around the double bond are responsible for significant restriction of rotational freedom of the Erg C20–C22 and C23–C24 bonds. The stabilization of the Erg β-angle (C17–C20–C22–C23) at ~240° further results in maintaining the *trans* conformation (180°) of the α-angle (C14–C17–C20–C22), which is a major determinant of the chain deviation from the direction of the ring system longest principal axis (the value of 180° means the colinear arrangement). The presence of the C26 methyl group in the Erg molecule also prevent free rotation around the C24–C25 bond (rotation of the isopropyl group), which is totally allowed in Chol.

To sum up, the chemical constitution of the Erg side chain determines the strong conformational stiffening of the examined part of molecule. Moreover, this rigid, bulky substituent can be recognized to some extent as a colinear extension of the steroid nucleus. The 2-isooctyl chain of Chol behaves in a completely different manner because, in fact, it exhibits a significant character of saturated hydrocarbon chain. This chain fragment is reasonably flexible and conformationally unstable; it also often deviates strongly from the direction of the ring system axis (see also Fig. 6). Ordering of lipid acyl chains usually occurs upon their contact with smooth and rigid molecular surfaces as a result of maximization of intermolecular van der Waals interactions (see also Intermolecular Interactions). Therefore, it seems to be obvious that conformational differences observed for the two types of sterols can underlie their different effect on structure and dynamics of the phospholipid acyl chains.

Surface structure

To better investigate the influence of sterols on a structure of the water/membrane interface, we calculated the distributions of the angle between the vector connecting P and N atoms from the DMPC headgroup and the bilayer normal (Fig. 8). The average value of the defined angle in the pure DMPC membrane (78.3°) is consistent with the experimental data (59), indicating that the P→N vectors tend to align with the bilayer plane. There is, however, a small inclination toward the water phase producing a nonzero component of the dipole moment in the direction perpendicular to the surface. Clearly, both sterols change the orientation of the P→N vectors in a similar way, making the distribution considerably wider. This flattening presumably results from two inverse effects caused by the presence of sterols. The decrease of the average area per phospholipid leads to the reduction of the in-plane component of the P→N dipole. On the contrary, one may observe a tendency of the DMPC headgroups to interact with the hydroxyl groups of the adjacent sterol molecules, which is accompanied by pointing the P→N vector toward the membrane center. The resulting distributions and average values of the studied angles (77.7° and 79.5° in the DMPC/Chol and DMPC/Erg system, respectively) differ from the previous data obtained for

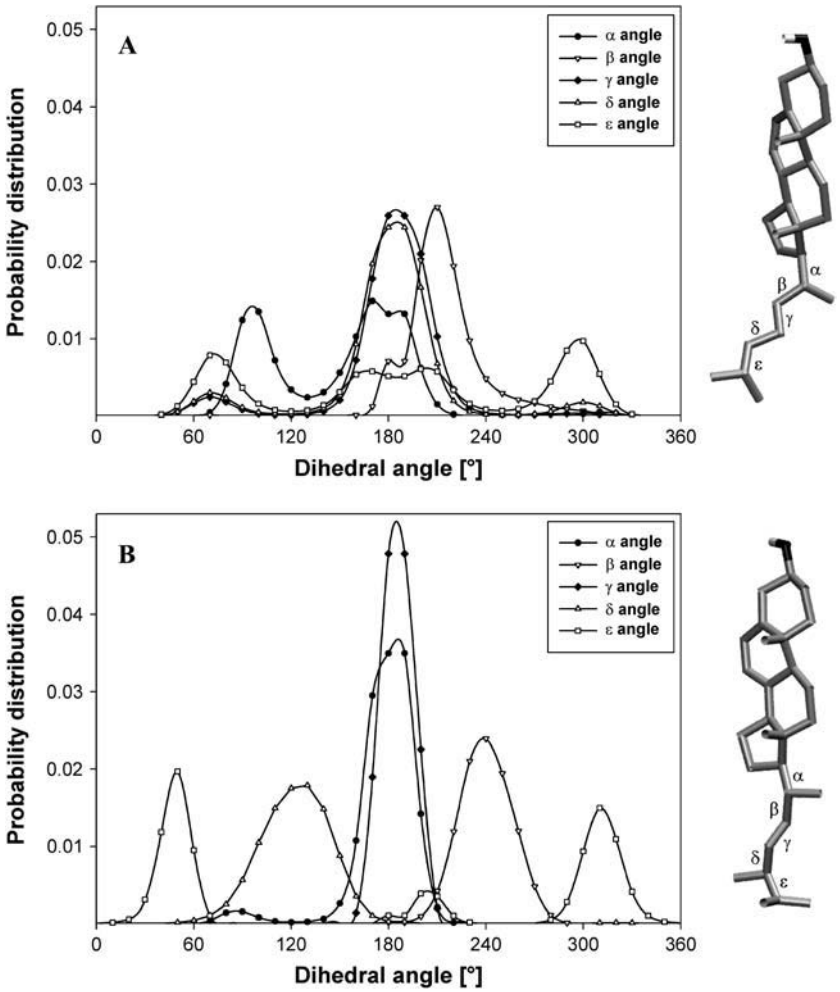

FIGURE 7 Distributions of the selected dihedral angles in the Chol (*a*) and Erg (*b*) side chains. Additionally, schematic images of sterol molecules were shown next to the corresponding plots.

DPPC bilayer containing 40 mol % of Chol, where the headgroups were directed more inwardly (31). This discrepancy may be a direct result of the different sterol contents in the both simulations. The sterol concentration of ~25 mol % is sufficient to induce the phase transition of a bilayer to the *lo* state (reducing the area per molecule); however, this amount is apparently too small to involve the majority of the DMPC headgroups in the direct interaction.

Three-dimensional radial distribution functions (RDF) of the chosen atoms around the nitrogen atom of DMPC molecules (Fig. 9) also confirm that, regardless of the type of sterol, the organization of the interfacial region in both mixed membranes is very similar. The locations and the widths of the related peaks in the RDFs calculated for both sterol systems are almost the same. A sharp maximum of probability at ~0.5 nm corresponds to the favorable electrostatic interaction between oppositely charged $N(CH_3)_3^+$ and PO_4^- groups from different DMPC molecules. The presence of a distinct peak in the RDF of the N-O pair (atom O comes from the sterol hydroxyl group) at ~0.45 nm verifies the occurrence of specific interaction between the DMPC headgroup (namely $N(CH_3)_3^+$) and the sterol 3β-hydroxyl group. By integrating these RDFs to the first minimum (i.e., calculating the area under the first peak), we established that one DMPC molecule, on average, participates in such interactions with ~0.3 sterol molecules. This amount is approximately equal to the sterol/DMPC concentration ratio in our systems, namely 0.33. Thus, it suggests that nearly all sterol molecules are involved in this kind of interaction, which is interpreted by some authors as a special type of hydrogen bond, where strongly polarized C atoms of the methyl groups (from $N(CH_3)_3^+$) may act as hydrogen donors (31). Comparing the RDF plots for the pure and sterol-containing bilayers, it seems that addition of ~25 mol % of Chol and Erg to a DMPC bilayer has roughly no effect on the optimal distances between the charged groups interacting within the membrane interface. Also, the average number of direct contacts between the $N(CH_3)_3^+$ and PO_4^- groups from different molecules (calculated as the area under the relevant peaks in Fig. 9) is nearly the same, and equals to ~2 in all three systems—indicating that a similar network of the charge pairs is present, irrespective of the phase state and the sterol

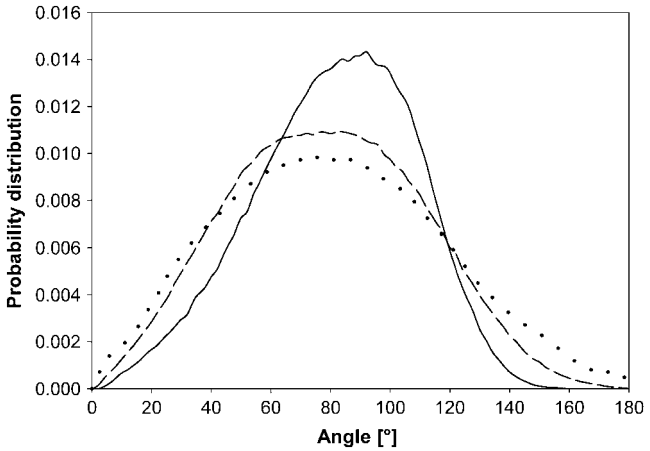

FIGURE 8 Distribution of the angle between P→N vector and the bilayer normal in the simulated systems: pure DMPC (*solid line*), DMPC/Chol (*dashed line*), and DMPC/Erg (*dotted line*).

type. These results are consistent with the experimental data, suggesting that sterol molecules have a rather minor effect on the membrane surface structure (60).

Translational diffusion

To quantitatively compare both sterol influence on the lateral (in plane of the membrane) and transversal (along the bilayer normal) diffusion of phospholipid molecules, we calculated the relevant diffusion constants, D, using Einstein equation

$$D = \lim_{t\to\infty} \frac{1}{2n}\frac{d}{dt}\langle[\mathbf{r}(t+t_0) - \mathbf{r}(t_0)]^2\rangle, \quad (4)$$

where $\mathbf{r}$ is the position of the center-of-mass (COM) of a molecule and n is the dimensionality of the motion. The averaging was done over all molecules and all possible time origins, t_0. The long-time slope of the mean-square displacement was estimated by fitting a straight line to the last five nanoseconds of each calculated relationship. To prevent overestimation, the diffusion constants were computed for each monolayer separately after removing the COM motion of the whole leaflet and then averaged. The results obtained for distinct D coefficients are shown in Table 1. It is evident that both Chol and Erg slow down the lateral diffusion of DMPC molecules in a significant way. This effect, which was previously shown in several experimental and computational studies (30,61,62), is believed to arise from the increased molecular order and closer packing of phospholipid molecules in the presence of sterols. The values of the lateral diffusion constants for the pure DMPC and DMPC/Chol bilayers estimated by us is quite consistent with the experimental data. For example, in a recent study employing pulse-field gradient NMR technique, the authors found that adding 25 mol % of Chol to the DMPC bilayer at 298 K resulted in decreasing of the lateral diffusion coefficient of DMPC from a value of 6.0

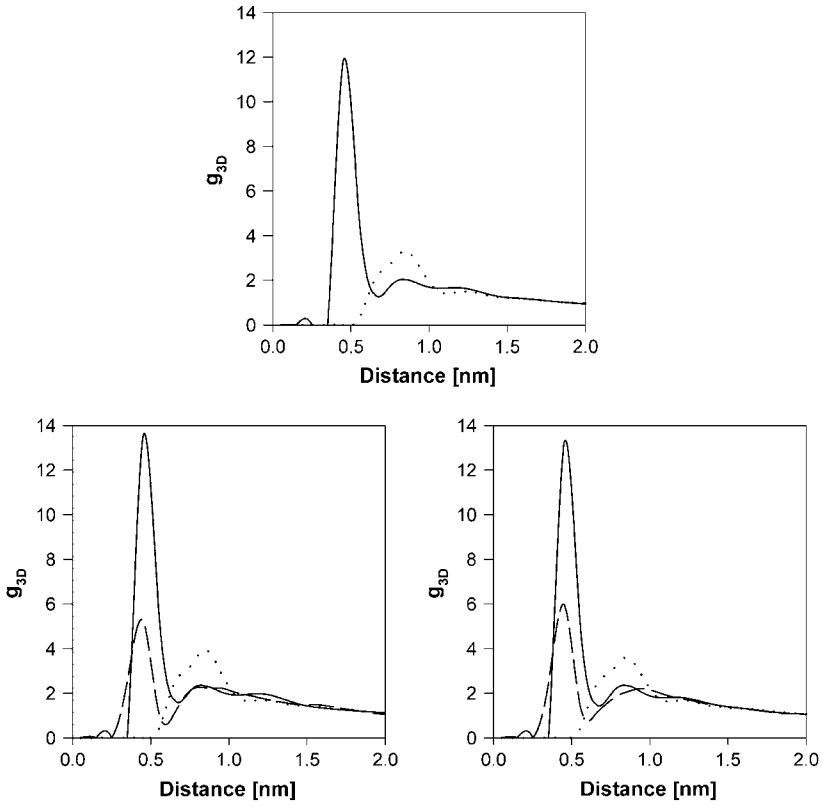

FIGURE 9 Radial distribution functions between the DMPC nitrogen atom and selected atoms from other molecules calculated in pure DMPC (*a*), DMPC/Chol (*b*), and DMPC/Erg (*c*) systems; DMPC phosphorus atom (*solid line*), hydrogen atom in the sterol hydroxyl group (*dashed line*), DMPC nitrogen atom (*dotted line*).

TABLE 1 Lateral (in the *x,y* plane) and transverse (along the *z* axis) diffusion coefficients calculated using Einstein's equation

Diffusion constant [10^{-8} cm^2/s]		Pure DMPC	DMPC/Chol	DMPC/Erg
DMPC	Lateral	11.0 ± 1.5	5.0 ± 0.73	2.0 ± 0.46
	Transverse	4.0 ± 0.46	2.0 ± 0.21	0.5 ± 0.23
Sterol	Lateral		6.0 ± 1.79	2.0 ± 1.56
	Transverse		2.0 ± 0.63	~0

$\times$ 10^{-8} to 3.0 $\times$ 10^{-8} cm^2/s (62). Additionally, our calculations show that, compared to Chol, Erg appears to more strongly restrict the lateral motion rate of phospholipids. This result is probably due to greater condensation and higher molecular order in the Erg-induced *lo* phase. Analysis of the COM *x*,*y* trajectories of the DMPC molecules (data not shown) suggests that tight molecular packing in the sterol systems may be considered both: 1), a factor reducing the amplitude of the molecule rattling-motion in a cage formed by its nearest-neighbors; and 2), a main reason for increasing of the cage-to-cage hopping activation barrier, which was manifested in the decrease of jump events along individual trajectories. The special caution should be paid when discussing calculated transversal diffusion constants. First of all, in equilibrated membrane systems these coefficients should be essentially equal to zero, otherwise the lipid bilayer would not be a stable structure. Nonzero values obtained for the pure DMPC and DMPC/Chol systems most probably arise from relatively short simulation time, which was not sufficient to appropriately sample the long-scale thickness fluctuations. Thus, the differences between transversal diffusion constants, determined for the three studied systems (Table 1), can be merely regarded as an approximate measure of the general effect of reducing thickness fluctuations with increasing internal order of the membrane. It should be also mentioned here that because lateral diffusion and long-scale collective phenomena as thickness fluctuations are (at least partially) independent, nonequilibrium state with respect to the latter process does not preclude obtaining a reasonable description of the former. In fact, many previous studies showed that even in relatively short simulations (nanosecond timescale), it is possible to gain lateral diffusion constants that are quantitatively consistent with experimental results (30).

We further analyzed translational motions of sterol molecules. Calculated diffusion constants (Table 1) are rather close, but in all cases slightly higher than corresponding ones obtained for DMPC. Concerning the smaller mass and more compact structure of sterols, one could postulate that similar rate of translational diffusion of the phospholipid and sterol molecules imply that possibly they are bound through majority of time and diffuse together (see also Intermolecular Interactions). The values of the lateral diffusion coefficients for both sterols are rather consistent with the results of the experimental studies on 6:4 DPPC/sterol mixed bilayers employing quasi-elastic neutron scattering, which at 36°C yielded values of 13.5 ± 3.6 $\times$ 10^{-8} and 3.5 ± 1.5 $\times$ 10^{-8} cm^2/s for Chol and Erg, respectively (20). Our simulations also reflected the difference in transversal mobility of both sterols. However, the calculated values of corresponding diffusion coefficients are one order-of-magnitude lower than the measured ones (20). Partially, this discrepancy can be due to the different length of the phospholipid acyl chains used in both studies. The DMPC used in our calculations, being shorter and better matched to the sterol molecules length, is likely to restrict their transverse mobility more effectively than DPPC used in Endress et al. (20).

Intermolecular interactions

Some of our previous findings (mentioned above) suggested the presence of strong hydrogen-bonding interactions between sterol and phospholipid molecules. Therefore, we attempted to compare the ability of both sterols to form such bonds. Employing typical geometric criterion for presence of a hydrogen bond (the distance between donor D and acceptor A is shorter than 0.35 nm, and the angle between the vector connecting D with A and the bond D–H is smaller than 60°) we calculated the average number of bonds formed between the sterol hydroxyl group and different accepting sites of DMPC molecules. The results, presented in Table 2, indicate that in both systems sterol hydroxyl groups form, on the average, almost one hydrogen bond with DMPC molecules. We can also see a significant preference for the carbonyl group of the *sn*-2 acyl chain. Quantitative analysis of hydrogen bonds revealed that both the number of the

TABLE 2 Nonbonded interactions between sterol and DMPC molecules

Average number of hydrogen bonds per sterol molecule				
DMPC group:	Cholesterol		Ergosterol	
Carbonyl *sn*-1	0.14 ± 0.05		0.11 ± 0.05	
Carbonyl *sn*-2	0.69 ± 0.04		0.82 ± 0.07	
PO_4^-	0.08 ± 0.03		0.03 ± 0.02	
Average van der Waals interaction energy per sterol molecule [kJ/mol]				
DMPC chains:	Cholesterol		Ergosterol	
	Ring system	Side chain	Ring system	Side chain
sn-1	−62.8 ± 1.66	−33.8 ± 1.18	−63.8 ± 1.94	−31.3 ± 1.54
sn-2	−64.0 ± 1.92	−27.8 ± 1.30	−70.0 ± 1.93	−28.7 ± 1.30

examined bonds and the observed preference were higher in the more ordered Erg-containing system. It seems that sterols prefer the *sn*-2 carbonyl interaction mode because binding to this acceptor, which is positioned closer to the surface than the *sn*-1carbonyl, guarantees the favorable location of the hydroxyl group within more polar and hydrated region of the lipid bilayer. On the other hand, direct interaction with the phosphate group leads to a substantial exposure of the sterol hydrophobic surface to water. A comparison of the length and angle distributions of the observed hydrogen bonds in both systems did not show any significant differences, thus a higher selectivity of bonds formed by Erg is probably due to its lower transverse mobility. In general, lengths of both sterol molecules and the DMPC acyl chains are very similar. This matching limits the amplitude of sterol transverse motion in DMPC/sterol membranes and may be a main reason for the higher number of sterol-phospholipid hydrogen bonds compared with the DPPC/Chol bilayer, in which case only ~0.7 bonds per the Chol molecule were observed (30).

Maximization of van der Waals intermolecular interaction energy due to straightening of the lipid acyl chains on the smooth molecular surface of the rigid sterol molecules is known to be a key process in the sterol-induced ordering of the chains. To get more details about the mechanism of the acyl-chain ordering we also analyzed the relevant van der Waals interactions. It turned out that the average energy of Lennard-Jones (LJ) interaction between sterol and the surrounding lipid acyl chains (i.e., interaction sites corresponding to all CH_2 and CH_3 groups of the DMPC chains) was similar in the two simulated systems (−188.4 and −193.8 kJ/mol per Chol and Erg molecule, respectively). However, these energy values should be treated with caution since they do not have any direct physical meaning and should be regarded rather as a measure of intermolecular contact within the studied systems. Knowing that the LJ energy, in our case, is roughly proportional to the number of interacting atoms, we could furthermore subtract from the value obtained for Erg, the energy of LJ interaction between an additional methyl group of the side chain and the DMPC acyl chains. As a result, we get a value of −187.7 kJ/mol which is almost the same as in the case of Chol, implying a similar contact surface between the two sterols and the hydrocarbon chains. Decomposition of the calculated van der Waals energies into contributions coming from interactions between the sterol rigid ring system or side chain and the two DMPC acyl chains treated separately (Table 2) reveals certain differences between both systems. The relatively stronger interaction of the Erg nucleus with the hydrocarbon chains is fully consistent with the higher molecular order and the tighter packing previously found in this system. Taking into account the similar structure of both sterol ring systems and their similar localization within the membrane, it could be argued that the difference in their interactions is due to more extensive reduction of free volume in this particular bilayer region in the case of the Erg-containing system. This result of the bilayer condensation was suggested to be, among other effects, an essential reason for the sterol-induced decreasing of the membrane permeability (63). For both sterols, the rigid nuclei interact more strongly with the *sn*-2 than with the *sn*-1 acyl chain, which is most probably a direct consequence of the observed hydrogen-bonding selectivity. This effect is especially evident in the case of Erg, which was found to exhibit a higher preference for the *sn*-2 carbonyl group. Closer to the bilayer midplane, we can see an opposite tendency—namely, that the energy of the LJ interaction between the sterol side chain and the *sn*-1 chain is in both systems higher than the contribution calculated for the *sn*-2 chain. This effect is probably due to the previously mentioned difference in the average position of both tails on the *z* axis. The *sn*-1 chain is located ~0.15 nm closer to the membrane midplane and, therefore, is able to develop a larger contact surface with the sterol side chain. The total energies of the sterol side-chain interactions with the phospholipid chains are similar in both systems. However, the value for Chol is a little higher, probably because this molecule contains the flexible isooctyl substituent that can more easily adjust to the elastic ends of the acyl chains, which tend to be in a disordered state. If we take into consideration the formerly established difference in the conformational freedom of the sterol side chains, the comparable interaction energies and, consequently, quite similar contact surfaces between the side chains and the acyl chains imply a major difference in the ordering ability of both sterols in this membrane region. This actually means that stiffer Erg side chain, being the majority of the time oriented along the bilayer normal, must induce stronger ordering and stretching of the neighboring lipid chains. It is also worth noticing that in the central bilayer region Erg interacts more strongly with the *sn*-2 chain than Chol does. This general tendency is also visible in Fig. 5, where difference in the ordering of the *sn*-2 chain in both type of sterol-containing membranes is higher than for the *sn*-1 chains.

We also investigated differences in hydration level of the interfacial region of all three simulated systems. Using the same criterion for the hydrogen bonding as before, we found that DMPC makes, on average, 6.5 ± 0.14, 6.0 ± 0.11, and 6.0 ± 0.12 bonds with surrounding water molecules in the pure DMPC, DMPC/Chol, and DMPC/Erg systems, respectively. Apparently, the addition of 25 mol % of sterols to the bilayer is accompanied by a slight decrease in headgroup hydration, most likely caused by the bilayer condensation that partially restricts water penetration into the membrane. The obtained numbers of hydrogen bonds are slightly higher than observed in experiment (64) and in simulation (65), probably as a result of using less strict criterion for hydrogen-bond presence.

To better characterize the DMPC solvation patterns in the examined systems, we calculated the three-dimensional RDFs of the water oxygen around the chosen atoms of

phospholipid molecules. By integrating these RDFs to the first minimum, we achieved the average number of water molecules in the first hydration layer around the given functional group (Table 3). It can be seen that the differences are rather minor, which actually is in agreement with the previous findings that sterols do not induce serious rearrangements of the membrane surface structure, and that the interface organization of both sterol-containing bilayers in *lo* phase is almost the same. These conclusions are also supported by a very similar shape of the corresponding RDF curves (calculated for different pair of atoms) in all three systems (data not shown). The small differences in solvation pattern of pure lipid bilayer and the bilayer containing sterols consist of the enhanced hydration of the *sn*-1 carbonyl and $N(CH_3)_3^+$ groups. The diversified exposure of the *sn*-1 carbonyl to water in the pure *ld* phase and in the sterol-containing *lo* phases seems to indicate that the membrane ordering is accompanied by widening the difference in relative localization of both carbonyl groups in the *z* axis. The partial dehydration of the $N(CH_3)_3^+$ groups in the sterol systems is, in turn, connected with the involvement of these groups in the direct interactions with the sterol hydroxyl groups. We believe that these interactions prevent also the increased penetration of the water molecules into the interface that could be expected as a result of incorporation of the relatively small sterol headgroups into the membrane surface. The hydration of the polar sterol headgroups was found to be similar for both types of sterols. Probably, as a consequence of its stronger preference for *sn*-2 carbonyl groups, Erg formed, on average, a slightly higher number of hydrogen bonds with water (0.44 ± 0.084) than Chol does (0.40 ± 0.078).

CONCLUSIONS

To compare the effect of cholesterol and ergosterol on the properties of the phosphatidylcholine bilayer, three molecular dynamics simulations were carried out: 1), the pure DMPC bilayer; 2), the DMPC bilayer containing ~25 mol % of Chol; and 3), the DMPC bilayer containing ~25 mol % of Erg. We believe that the length of all simulations was sufficient to reach equilibrium and obtain reasonable convergence of all properties that were of our interest. This revealed various molecular properties of studied systems, and especially Erg-containing membranes, previously reported only experimentally as macroscopic observations.

TABLE 3 Average number of water molecules in the first hydration layer calculated by integrating the corresponding RDFs

DMPC group	Pure DMPC	DMPC/Chol	DMPC/Erg
$N(CH_3)_3^+$	22.4	19.4	18.5
PO_4^-	7.0	6.9	7.0
C=O (*sn*-1)	0.8	0.5	0.6
C=O (*sn*-2)	1.7	1.8	1.7

In our studies, Erg was found to decrease the area per one DMPC lipid molecule, and to increase lipid acyl-chain order, as well as the bilayer thickness, to a greater extent than Chol. This finding is consistent with a number of previously reported experimental studies (14–17). This work, however, demonstrates this effect at the molecular level, enabling us to recognize the putative reason for the observed difference. On the basis of various analyses we concluded that the main cause of Erg's higher ability to increase lipid molecular order is the restricted conformational freedom of its side-chain moiety resulting from the presence of the double bond and the additional methyl group. It is worth noticing that greater conformational flexibility of Chol side chain was also observed for isolated sterol molecules (43). This means that lipid environment does not strongly influence the side-chain flexibility and the observed difference stems directly from different structure of both sterols. On the other hand, vertically oriented and more rigid Erg side chains effectively order (straight up) fragments of lipid acyl chains located closer to the membrane midplane. This ordering effect caused by sterol side chain propagates in the whole bilayer.

We also established that both sterols exert very similar and rather minor influence on the water/bilayer interface structure. Specifically, it was found that, upon addition of sterol, the phospholipid $N(CH_3)_3^+$ groups were engaged in the direct interaction with the sterol polar headgroups. This effect is recognized by some authors as an important step necessary for the formation of sterol/phospholipid complexes (31).

Our results also support the experimental data on reducing the lipid translational diffusion constants in the sterol-induced *lo* phases (61,66). Moreover, we showed that this decrease is greater in the case of the more ordered Erg-containing membrane. In comparison with Chol, Erg exhibits noticeably higher preference for making a hydrogen bond with *sn*-2 carbonyl group of DMPC which, in turn, causes stronger interaction with the *sn*-2 hydrocarbon chain and relatively better ordering of this particular acyl chain in the Erg-containing system.

It is generally accepted that modulation of the lipid bilayer physicochemical properties by Chol and especially its ability to promote the emergence of the membrane *lo* state determines a biological importance of this sterol (3,22). The qualitatively similar influence of Erg on the DMPC bilayer behavior, observed in our simulations, indicates that the fungal sterol may have a comparable effect on such properties of the biological membranes as elastomechanical strength, fluidity, and permeability. On the other hand, the difference found by us in the ordering ability of both sterols seems to explain the significantly stronger Erg activity in promotion of ordered lipid domains (rafts) that was established experimentally by the fluorescence quenching and detergent insolubility methods (67). Our results support, therefore, the

conjecture that the domain-promoting activity depends especially on the ability to increase the chain ordering of saturated lipids such as many naturally occurring glycero- and sphingolipids. Maximal stretching and orientation along the bilayer normal of the Erg side chain may also be of a special importance for ordering the specific fungal sphingolipids that possess unusually long amide chains (C26:0).

In the context of the polyene antibiotics mechanism of action, quantitative differences in the molecular order of both simulated sterol-induced *lo* phases could be postulated as a factor that plays a major role in providing a selective toxicity of the antibiotic. Such a hypothesis of indirect sterol action is supported by some experimental studies (68) and our preliminary calculations (to be published elsewhere) showing that molecular order of the lipid bilayer, to a large extent, determines the antibiotic molecule orientation in the membrane and may, therefore, influence its ability to self-aggregate and form a functional ion channel.

The work was supported in part by grant No. 3 P05F 012 25 from the Ministry of Science and Information Technology (Poland) and in part by internal grants from Gdansk University of Technology (Poland). The authors also thank TASK Computational Center (Gdansk, Poland) for granting CPU time.

REFERENCES

1. Yeagle, P. L., A. D. Albert, K. Boesze-Battaglia, J. Young, and J. Frye. 1990. Cholesterol dynamics in membranes. *Biophys. J.* 57:413–424.
2. Simons, K., and E. Ikonen. 2000. Cell biology—how cells handle cholesterol. *Science.* 290:1721–1726.
3. McMullen, T. P. W., and R. N. McElhaney. 1996. Physical studies of cholesterol-phospholipid interactions. *Curr. Opin. Colloid Interface Sci.* 1:83–90.
4. Ohvo-Rekila, H., B. Ramstedt, P. Leppimaki, and J. P. Slotte. 2002. Cholesterol interactions with phospholipids in membranes. *Prog. Lipid Res.* 41:66–97.
5. Trouard, T. P., A. A. Nevzorov, T. M. Alam, C. Job, J. Zajicek, and M. F. Brown. 1999. Influence of cholesterol on dynamics of dimyristoylphosphatidylcholine bilayers as studied by deuterium NMR relaxation. *J. Chem. Phys.* 110:8802–8818.
6. Barenholz, Y. 2002. Cholesterol and other membrane active sterols: from membrane evolution to ''rafts''. *Prog. Lipid Res.* 41:1–5.
7. Vist, M. R., and J. H. Davis. 1990. Phase equilibria of cholesterol/dipalmitoylphosphatidylcholine mixtures: deuterium nuclear magnetic resonance and differential scanning calorimetry. *Biochemistry.* 29: 451–464.
8. Simons, K., and E. Ikonen. 1997. Functional rafts in cell membranes. *Nature.* 387:569–572.
9. Edidin, M. 2003. The state of lipid rafts: from model membranes to cells. *Annu. Rev. Biophys. Biomol. Struct.* 32:257–283.
10. Lafont, F., and F. G. Van der Goot. 2005. Bacterial invasion via lipid rafts. *Cell Microbiol.* 7:613–620.
11. Brown, D. A., and E. London. 1998. Functions of lipid rafts in biological membranes. *Annu. Rev. Cell Dev. Biol.* 14:111–136.
12. Bloch, K. 1981. Sterol structure and membrane function. *Curr. Top. Cell. Regul.* 18:289–299.
13. Mouritsen, O. G., and M. J. Zuckermann. 2004. What's so special about cholesterol? *Lipids.* 39:1101–1113.
14. Urbina, J. A., S. Pekerar, L. Hong-biao, J. Patterson, B. Montez, and E. Oldfield. 1995. Molecular order and dynamics of phosphatidylcholine bilayer membranes in the presence of cholesterol, ergosterol and lanosterol: a comparative study using ^{2}H-, ^{13}C- and ^{31}P-NMR spectroscopy. *Biochim. Biophys. Acta Biomembr.* 1238:163–176.
15. Endress, E., S. Bayerl, K. Prechtel, C. Maier, R. Merkel, and T. M. Bayerl. 2002. The effect of cholesterol, lanosterol, and ergosterol on lecithin bilayer mechanical properties at molecular and microscopic dimensions: a solid-state NMR and micropipette study. *Langmuir.* 18:3293–3299.
16. Bernsdorff, C., and R. Winter. 2003. Differential properties of the sterols cholesterol, ergosterol, β- sitosterol, trans-7-dehydrocholesterol, stigmasterol and lanosterol on DPPC bilayer order. *J. Phys. Chem. B.* 107:10658–10664.
17. Hsueh, Y. W., K. Gilbert, C. Trandum, M. Zuckermann, and J. Thewalt. 2005. The effect of ergosterol on dipalmitoylphosphatidylcholine bilayers: a deuterium NMR and calorimetric study. *Biophys. J.* 88:1799–1808.
18. Bagnat, M., S. Keranen, A. Shevchenko, A. Shevchenko, and K. Simons. 2000. Lipid rafts function in biosynthetic delivery of proteins to the cell surface in yeast. *Proc. Natl. Acad. Sci. USA.* 97:3254–3259.
19. Rietveld, A., S. Neutz, K. Simons, and S. Eaton. 1999. Association of sterol- and glycosylphosphatidylinositol-linked proteins with *Drosophila* raft lipid microdomains. *J. Biol. Chem.* 274:12049–12054.
20. Endress, E., H. Heller, H. Casalta, M. F. Brown, and T. M. Bayerl. 2002. Anisotropic motion and molecular dynamics of cholesterol, lanosterol, and ergosterol in lecithin bilayers studied by quasi-elastic neutron scattering. *Biochemistry.* 41:13078–13086.
21. Wang, J. W., and L. E. Megha. 2004. Relationship between sterol/steroid structure and participation in ordered lipid domains (lipid rafts): implications for lipid raft structure and function. *Biochemistry.* 43: 1010–1018.
22. Miao, L., M. Nielsen, J. Thewalt, J. H. Ipsen, M. Bloom, M. J. Zuckermann, and O. G. Mouritsen. 2002. From lanosterol to cholesterol: structural evolution and differential effects on lipid bilayers. *Biophys. J.* 82:1429–1444.
23. Nielsen, M., J. Thewalt, L. Miao, J. H. Ipsen, M. Bloom, M. J. Zuckermann, and O. G. Mouritsen. 2000. Sterol evolution and the physics of membranes. *Europhys. Lett.* 52:368–374.
24. Tieleman, D. P., S. J. Marrink, and H. J. C. Berendsen. 1997. A computer perspective of membranes: molecular dynamics studies of lipid bilayer systems. *Biochim. Biophys. Acta Rev. Biomembr.* 1331: 235–270.
25. Feller, S. E. 2000. Molecular dynamics simulations of lipid bilayers. *Curr. Opin. Colloid Interface Sci.* 5:217–223.
26. Scott, H. L. 2002. Modeling the lipid component of membranes. *Curr. Opin. Struct. Biol.* 12:495–502.
27. Tu, K. C., M. L. Klein, and D. J. Tobias. 1998. Constant-pressure molecular dynamics investigation of cholesterol effects in a dipalmitoylphosphatidylcholine bilayer. *Biophys. J.* 75:2147–2156.
28. Pasenkiewicz-Gierula, M., T. Rog, K. Kitamura, and A. Kusumi. 2000. Cholesterol effects on the phosphatidylcholine bilayer polar region: a molecular simulation study. *Biophys. J.* 78:1376–1389.
29. Chiu, S. W., E. Jakobsson, R. J. Mashl, and H. L. Scott. 2002. Cholesterol-induced modifications in lipid bilayers: a simulation study. *Biophys. J.* 83:1842–1853.
30. Hofsass, C., E. Lindahl, and O. Edholm. 2003. Molecular dynamics simulations of phospholipid bilayers with cholesterol. *Biophys. J.* 84: 2192–2206.
31. Pandit, S. A., D. Bostick, and M. L. Berkowitz. 2004. Complexation of phosphatidylcholine lipids with cholesterol. *Biophys. J.* 86:1345–1356.
32. Smondyrev, A. M., and M. L. Berkowitz. 2001. Molecular dynamics simulation of the structure of dimyristoylphosphatidylcholine bilayers with cholesterol, ergosterol, and lanosterol. *Biophys. J.* 80:1649–1658.
33. Bolard, J. 1986. How do the polyene macrolide antibiotics affect the cellular membrane properties? *Biochim. Biophys. Acta.* 864:257–304.
34. Paquet, M. J., I. Fournier, J. Barwicz, P. Tancrede, and M. Auger. 2002. The effects of amphotericin B on pure and ergosterol- or

cholesterol-containing dipalmitoylphosphatidylcholine bilayers as viewed by H-2 NMR. *Chem. Phys. Lipids.* 119:1–11.

35. Coutinho, A., and M. Prieto. 2003. Cooperative partition model of nystatin interaction with phospholipid vesicles. *Biophys. J.* 84:3061–3078.
36. Rog, T., and M. Pasenkiewicz-Gierula. 2003. Effects of epicholesterol on the phosphatidylcholine bilayer: a molecular simulation study. *Biophys. J.* 84:1818–1826.
37. Rog, T., and M. Pasenkiewicz-Gierula. 2004. Nonpolar interactions between cholesterol and phospholipids: a molecular dynamics simulation study. *Biophys. Chem.* 107:151–164.
38. Baginski, M., H. Resat, and J. A. McCammon. 1997. Molecular properties of amphotericin B membrane channel: a molecular dynamics simulation. *Mol. Pharmacol.* 52:560–570.
39. Baginski, M., H. Resat, and E. Borowski. 2002. Comparative molecular dynamics simulations of amphotericin B—cholesterol/ergosterol membrane channels. *Biochim. Biophys. Acta Biomembr.* 1567:63–78.
40. Sternal, K., J. Czub, and M. Baginski. 2004. Molecular aspects of the interaction between amphotericin B and a phospholipid bilayer: molecular dynamics studies. *J. Mol. Model.* (*Online*). 10:223–232.
41. Shieh, H. S., L. G. Hoard, and C. E. Nordman. 1981. The structure of cholesterol. *Acta Crystallogr. B.* 37:1538–1543.
42. Hull, S. E., and M. M. Woolfson. 1976. The crystal structure of ergosterol monohydrate. *Acta Crystallogr. B.* 32:2370–2373.
43. Baginski, M., A. Tempczyk, and E. Borowski. 1989. Comparative conformational analysis of cholesterol and ergosterol by molecular mechanics. *Eur. Biophys. J.* 17:159–166.
44. Berendsen, H. J. C., D. van der Spoel, and R. van Drunen. 1995. GROMACS: a message-passing parallel molecular dynamics implementation. *Comput. Phys. Comm.* 91:43–56.
45. Berger, O., O. Edholm, and F. Jahnig. 1997. Molecular dynamics simulations of a fluid bilayer of dipalmitoylphosphatidylcholine at full hydration, constant pressure, and constant temperature. *Biophys. J.* 72:2002–2013.
46. Baginski, M., and E. Borowski. 1997. Distribution of electrostatic potential around amphotericin B and its membrane targets. *Theochem. J. Mol. Struct.* 389:139–146.
47. Berendsen, H. J. C., J. P. M. Postma, W. F. van Gunsteren, and J. Hermans. 1981. Interaction models in relation to protein hydration. *In* Intermolecular Forces. B. Pullman, editor. Riedel, Dordrecht, The Netherlands. 331–342.
48. Essmann, U., L. Perera, M. L. Berkowitz, T. Darden, H. Lee, and L. G. Pedersen. 1995. A smooth particle mesh Ewald method. *J. Chem. Phys.* 103:8577–8593.
49. Hess, B., H. Bekker, H. J. C. Berendsen, and J. G. E. M. Fraaije. 1997. LINCS: a linear constraint solver for molecular simulations. *J. Comput. Chem.* 18:1463–1472.
50. Miyamoto, S., and P. A. Kollman. 1992. SETTLE—an analytical version of the SHAKE and RATTLE algorithm for rigid water models. *J. Comput. Chem.* 13:952–962.
51. Berendsen, H. J. C., J. P. M. Postma, A. Dinola, and J. R. Haak. 1984. Molecular dynamics with coupling to an external bath. *J. Chem. Phys.* 81:3684–3690.
52. Petrache, H. I., S. Tristram-Nagle, and J. F. Nagle. 1998. Fluid phase structure of EPC and DMPC bilayers. *Chem. Phys. Lipids.* 95:83–94.
53. Nagle, J. F., and S. Tristram-Nagle. 2000. Structure of lipid bilayers. *Biochim. Biophys. Acta Rev. Biomembr.* 1469:159–195.
54. Falck, E., M. Patra, M. Karttunen, M. T. Hyvonen, and I. Vattulainen. 2004. Lessons of slicing membranes: interplay of packing, free area, and lateral diffusion in phospholipid/cholesterol bilayers. *Biophys. J.* 87:1076–1091.
55. Tristram-Nagle, S., Y. F. Liu, J. Legleiter, and J. F. Nagle. 2002. Structure of gel phase DMPC determined by x-ray diffraction. *Biophys. J.* 83:3324–3335.
56. Pastor, R. W., R. M. Venable, and S. E. Feller. 2002. Lipid bilayers, NMR relaxation, and computer simulations. *Acct. Chem. Res.* 35:438–446.
57. Kucerka, N., Y. Liu, N. Chu, H. I. Petrache, S. Tristram-Nagle, and J. F. Nagle. 2005. Structure of fully hydrated fluid phase DMPC and DLPC lipid bilayers using x-ray scattering from oriented multilamellar arrays and from unilamellar vesicles. *Biophys. J.* 88:2626–2637.
58. Petrache, H. I., S. W. Dodd, and M. F. Brown. 2000. Area per lipid and acyl length distributions in fluid phosphatidylcholines determined by ^{2}H NMR spectroscopy. *Biophys. J.* 79:3172–3192.
59. Akutsu, H., and T. Nagamori. 1991. Conformational analysis of the polar headgroup in phosphatidylcholine bilayers: a structural change induced by cations. *Biochemistry.* 30:4510–4516.
60. Brown, M. F., and J. Seelig. 1978. Influence of cholesterol on the polar region of phosphatidylcholine and phosphatidylethanolamine bilayers. *Biochemistry.* 17:381–384.
61. Almeida, P. F. F., W. L. C. Vaz, and T. E. Thompson. 1992. Lateral diffusion in the liquid phases of dimyristoylphosphatidylcholine/cholesterol lipid bilayers: a free volume analysis. *Biochemistry.* 31:6739–6747.
62. Filippov, A., G. Oradd, and G. Lindblom. 2003. Influence of cholesterol and water content on phospholipid lateral diffusion in bilayers. *Langmuir.* 19:6397–6400.
63. Corvera, E., O. G. Mouritsen, M. A. Singer, and M. J. Zuckerman. 1992. The permeability and the effect of acyl chain length for phospholipid bilayers containing cholesterol: theory and experiment. *Biochim. Biophys. Acta.* 1107:261–270.
64. Gawrisch, K., K. Arnold, T. Gottwald, G. Klose, and F. Volke. 1978. NMR studies of the phosphate-water interaction in dipalmitoylphosphatidylcholine-water system. *Stud. Biophysica.* 74:13–14.
65. Pasenkiewicz-Gierula, M., Y. Takaoka, H. Miyagawa, K. Kitamura, and A. Kusumi. 1999. Charge pairing of headgroups in phosphatidylcholine membranes: A molecular dynamics simulation study. *Biophys. J.* 76:1228–1240.
66. Filippov, A., G. Oradd, and G. Lindblom. 2003. The effect of cholesterol on the lateral diffusion of phospholipids in oriented bilayers. *Biophys. J.* 84:3079–3086.
67. Xu, X. L., R. Bittman, G. Duportail, D. Heissler, C. Vilcheze, and E. London. 2001. Effect of the structure of natural sterols and sphingolipids on the formation of ordered sphingolipid/sterol domains (rafts). *J. Biol. Chem.* 276:33540–33546.
68. Lopes, S., and M. A. R. B. Castanho. 2002. Revealing the orientation of Nystatin and Amphotericin B in lipidic multilayers by UV-VIS linear dichroism. *J. Phys. Chem. B.* 106:7278–7282.